Received: 12 November 2022 | Revised: 17 August 2023 | Accepted: 28 August 2023

DOI: 10.1002/hbm.26484

RESEARCH ARTICLE

WILEY

Spatiotemporal dedifferentiation of the global brain signal topography along the adult lifespan

Yujia Ao[1,2] | Chengxiao Yang[1] | Jan Drewes[1] | Muliang Jiang[3] | Lihui Huang[1] | Xiujuan Jing[1] | Georg Northoff[2] | Yifeng Wang[1]

[1]Institute of Brain and Psychological Sciences, Sichuan Normal University, Chengdu, China

[2]Mind, Brain Imaging and Neuroethics Research Unit, Institute of Mental Health Research, Faculty of Medicine, University of Ottawa, Ottawa, Ontario, Canada

[3]First Affiliated Hospital, Guangxi Medical University, Nanning, China

Correspondence
Yifeng Wang, Institute of Brain and Psychological Sciences, Sichuan Normal University, No. 5, Jing'an Road, Chengdu 610066, China.
Email: wyf@sicnu.edu.cn

Funding information
National Natural Science Foundation of China, Grant/Award Number: 62177035

Abstract

Age-related variations in many regions and/or networks of the human brain have been uncovered using resting-state functional magnetic resonance imaging. However, these findings did not account for the dynamical effect the brain's global activity (global signal [GS]) causes on local characteristics, which is measured by GS topography. To address this gap, we tested GS topography including its correlation with age using a large-scale cross-sectional adult lifespan dataset ($n = 492$). Both GS topography and its variation with age showed frequency-specific patterns, reflecting the spatiotemporal characteristics of the dynamic change of GS topography with age. A general trend toward dedifferentiation of GS topography with age was observed in both spatial (i.e., less differences of GS between different regions) and temporal (i.e., less differences of GS between different frequencies) dimensions. Further, methodological control analyses suggested that although most age-related dedifferentiation effects remained across different preprocessing strategies, some were triggered by neuro-vascular coupling and physiological noises. Together, these results provide the first evidence for age-related effects on global brain activity and its topographic-dynamic representation in terms of spatiotemporal dedifferentiation.

KEYWORDS
brain aging, fMRI, global signal topography, lifespan, spatiotemporal dedifferentiation

1 | INTRODUCTION

The human brain is a dynamic system that undergoes continuous change throughout the lifespan (Ferreira & Busatto, 2013; Lou et al., 2019; Vij et al., 2018; Xia et al., 2019), which can be measured in vivo by resting-state functional magnetic resonance imaging (rs-fMRI) (Ferreira & Busatto, 2013; Xia et al., 2019; Zuo et al., 2019). Using rs-fMRI, a host of studies have documented altered functional organization of spontaneous brain activity with age, such as increased or decreased functional connections (FCs) in almost all intrinsic functional networks (Ferreira & Busatto, 2013; Tian et al., 2018; Tomasi & Volkow, 2012; Vij et al., 2018). The widespread regional and network changes suggest a global alteration of brain activity in the aging brain.

Global brain activity can be measured by the global signal (GS), which is the mean of the whole brain blood oxygen level dependent (BOLD) signal (Power et al., 2014, 2017). Initially considered to be nonneuronal noise (Power et al., 2014, 2017, 2019), recent studies have demonstrated a close association between GS and neurobiological activities (Fox et al., 2009; Murphy & Fox, 2017) such as local field potentials (Schölvinck et al., 2010). The GS is manifested in different extents across various brain regions, resulting in GS topography, which is defined as the correlation between GS correlation (GSCORR)

and local signals (Yang et al., 2017). Recently, the GS topography has been suggested to be an essential marker of psychopathological symptoms, cognitive tasks, and consciousness states (Tanabe et al., 2020). Given that the aging brain is featured with universal neural and cognitive decline (Koen et al., 2020), GS topography may delineate global changes during brain aging, providing insights into the process of healthy aging and serving as the baseline of geriatric diseases.

In addition, the functional organization of brain networks is constrained by time scales from seconds (De Domenico et al., 2016; Wang, Zou, et al., 2020) to decades (Yang et al., 2013, 2018). In the short time scale, frequency-specific FC has been widely identified to be a core neurophysiological mechanism of brain function (Adaikkan et al., 2019; Buzsáki, 2006; Fiebelkorn & Kastner, 2019; Han et al., 2017; Perrault et al., 2019; Wang et al., 2016; Watrous et al., 2013). For example, frequency-specific alteration of the GS topography has been observed in patients with schizophrenia (Wang, Liao, et al., 2020). On the other hand, the human lifespan, as the largest time scale of dynamic brain development, dominates and changes the functional organization of the whole brain (Cao et al., 2014; Vij et al., 2018). Therefore, the frequency characteristics of GS topography across the adult lifespan are of importance for the global dynamics during brain aging.

The dedifferentiation hypothesis is a key theory of brain aging (Sala-Llonch et al., 2015), which proposes a loss of functional specificity of brain regions and more homogeneous neural responses (Koen et al., 2020; Koen & Rugg, 2019; Park et al., 2004). Research has shown that within-network FCs decrease with age, while between-network FCs increase, resulting in more homogeneous connectivity patterns across the entire brain (Damoiseaux, 2017; Malagurski et al., 2020). The GS topography has been identified as featuring differentiated GSCORR between unimodal and transmodal regions (Ao et al., 2021; Yang et al., 2017; Zhang et al., 2020). Previous research has demonstrated a diminution in the differences in GSCORR between sensory and association regions in individuals with schizophrenia, suggesting a psychiatric-related dedifferentiation (Yang et al., 2017). However, it remains uncertain whether an analogous spatial and temporal dedifferentiation, marked by reduced local-regional and dynamic frequency differences, can be observed in the GS topography of the aging brain. Such spatiotemporal dedifferentiation of global brain topography would provide further support on the neural level itself for the more cognitive- and function-based dedifferentiation hypothesis (Baltes & Lindenberger, 1997).

Drawing on our previous work (Ao et al., 2022), we aim to expand and bolster the notion of age-related spatiotemporal dedifferentiation by investigating the variation of the spatiotemporal organization of GS topography across the adult lifespan using a large-sample rs-fMRI dataset. In addition to the dedifferentiation across distributed brain regions, we have observed a more homogenous distribution of GS power spectrum density (PSD) across frequency bands in the aging brain (Ao et al., 2022). We thus hypothesized that the GSCORR would become more homogenous with age in different brain regions and frequency bands. To begin, we calculated the GS topography (GSCORR) using the magnitude-squared coherence, which captures FC in both spatial and temporal/frequency dimensions (De Domenico et al., 2016; Sasai et al., 2021). We then estimated Pearson's correlation between age and GS topography to elucidate the variability of GS topography with age (GS-TV). To measure the dedifferentiation of GS topography with age, we calculated the Pearson's correlation between GS-TV and GSCORR. If the dedifferentiation of GS topography is genuine, the correlation should be negative, with regions having high GSCORR decreasing with age and regions with low GSCORR increasing with age. On the contrary, the differentiation of GS topography occurs when there is a positive correlation. Given that the physiological factors including head motion, white matter, cerebrospinal fluid signals, and vascular components are frequently contested confounds in detecting BOLD signal in elderly individuals (Fabiani et al., 2014; Tarantini et al., 2017), we aim to investigate the contribution of these physiological factors to our findings. We have demonstrated our results both prior to and following the deconvolution of the hemodynamic response function (HRF) to scrutinize the contributions stemming from neurovascular coupling. Furthermore, we have applied varying control strategies to manage the influence of other physiological signals and have subsequently discussed their outcomes.

2 | MATERIALS AND METHODS

2.1 | Participants

All subjects in this study came from a public database: the International Data-sharing Initiative (http://fcon_1000.projects.nitrc.org/indi/retro/sald.html). A total of 492 healthy participants (308 females; ages ranged: 19–80 years) were recruited from Southwest University (SWU, Chongqing, China) through leaflets, online advertisements, campus social networks, and face-to-face propaganda (Wei et al., 2018). All participants were healthy, and had no history of psychiatric disorder or substance abuse (including illicit drugs and alcohol), or magnetic resonance imaging (MRI) contraindications. The project was approved by the Research Ethics Committee of the Brain Imaging Center of Southwest University, following the Declaration of Helsinki. Written informed consent was obtained from each participant before the data collection. Participants received payment depending on the time and tasks completed.

2.2 | Imaging data acquisition

All of the data were obtained from a 3T Siemens Trio MRI scanner (Siemens Medical, Erlangen, Germany) at the Brain Imaging Center of SWU. During the rs-fMRI scan, subjects were instructed to lie down, close their eyes, and rest without thinking about anything in particular but to refrain from falling asleep. The 8-min scan of 242 contiguous whole-brain functional images was acquired using a T2*-weighted gradient echo planar imaging (EPI) sequence: slices = 32, repetition time (TR)/echo time (TE) = 2000/30 ms, flip angle = 90°, field of

view = 220 mm × 220 mm, thickness = 3 mm, slice gap = 1 mm, resulting in voxels measuring 3.4 × 3.4 × 4 mm^3.

2.3 | Data preprocessing

The preprocessing of functional images was conducted using the "Data Processing Assistant for Resting-State fMRI" package (DPARSFA, http://www.restfmri.net) (Yan et al., 2016), according to the steps of previous studies (Fox et al., 2009; Wang, Liao, et al., 2019): removal of the first seven volumes, slice timing, and realignment. The corrected images were normalized to the standard EPI template and resampled to a 3 × 3 × 3 mm^3 voxel size. The linear trend, white matter, and cerebrospinal fluid signals were regressed out from the BOLD signals with default parameters in the DPARSFA software. To minimize the head motion factor, we further linearly regressed out Friston's 24 motion parameters, including 6 head motions, 6 temporal derivatives, and 12 corresponding squares, as well as "bad" time points, with mean framewise displacement (mean FD) >0.2 mm (Jenkinson et al., 2002), following previous studies (Satterthwaite et al., 2013; Yan et al., 2013). Note that we did not exclude subjects with high levels of mean FD or contaminated volumes, as doing so would introduce a bias in the sample by disproportionately excluding elder participants. Additionally, we noticed a correlation between an augmentation in head motion and aging ($r = 0.35$, $p < .0001$). We have chosen to document the GS-TV and its dedifferentiation with the individual mean FD regressed. This information is included in the Supporting Information for further reference. This decision was made on the basis that the aforementioned increase in head motion could potentially introduce distortions in the post-processed output, particularly after the effects of head motion have been mitigated during preprocessing.

2.4 | Blind HRF de-convolution

The neurovascular factor is an essential contributor to the BOLD signal, which undergoes changes with age (Fabiani et al., 2014; Tarantini et al., 2017). Different HRFs have been observed in brain aging, characterized by increased time-to-peak and decreased peak amplitude with age (West et al., 2019). In addition, the HRF can confound the temporal precedence estimation (Wu, Liao, et al., 2013), which could distort coherence analysis. Hence, we implemented the blind HRF de-convolution at the subject-level, to control the neurovascular factor and test its effect on the GS topography dedifferentiation. This method has demonstrated robustness, feasibility, and efficacy in eliminating neurovascular coupling effects in BOLD time series (Wang et al., 2023; Wu, Liao, et al., 2013; Wu et al., 2021).

Analogous to our previous studies (Ao et al., 2022; Wang et al., 2014, 2015), the following steps were conducted. After noise regression, a point process analysis was performed to detect spontaneous neural events. BOLD values exceeding the mean plus one standard deviation were extracted and the onsets of neural events were estimated and collected for HRF reconstruction (Wu et al., 2021; Wu, Stramaglia, et al., 2013). The BOLD signal was matched with the canonical HRF and its time derivative to get the HRF in each voxel. Finally, a Wiener de-convolution was applied to recover signals at the neural level (https://www.nitrc.org/projects/rshrf) (Wu, Liao, et al., 2013; Wu et al., 2021).

2.5 | GS topography measurements and its age-related effects

The GS was obtained by averaging BOLD signals over all voxels within the Human Brainnetome Atlas (Fan et al., 2016; Wang, Wang, et al., 2019). The GS topography was defined by the FC between the GS and the time course of each brain region constrained by the Human Brainnetome Atlas. We used the coherence method, which is based on frequency division and temporal correlation, to avoid the limitations of traditional FC (Chen et al., 2016; Wu et al., 2008). First, there is no consensus on the number of bands that the low frequency brain signal should be divided into due to insufficient knowledge about its psychophysiological meanings (Baria et al., 2011; Buzsáki & Draguhn, 2004; Krishnan et al., 2018). Furthermore, temporal correlation is sensitive to the phase of brain signals. If there is a fixed phase lag between two signals, an uncorrelated or even anticorrelated relationship may be uncovered by temporal correlation, even though there is information exchange between these signals (Fox et al., 2005; Murphy & Fox, 2017; Wang, Huang, et al., 2019). The coherence method overcomes these limitations by differentiating the full band into narrow frequency bins and is immune to phase lags when estimating temporal dependence (Li et al., 2015; Salvador et al., 2008; Wang, Huang, et al., 2019). Consistent with previous studies (De Domenico et al., 2016; Sasai et al., 2021; Wang et al., 2016), we used the coherence coefficient C to measure FC across the full frequency band as in Equation (1)

$$C(f) = \frac{P_{(roi,gs)}(f)}{\sqrt{P_{roi}(f) \times \sqrt{P_{gs}(f)}}}, \quad (1)$$

where $C(f)$ is the coherence coefficient at frequency f. P_{roi} and P_{gs} are PSDs of local signals and the GS estimated using Welch's fast Fourier transform (FFT) method and $P_{(roi,gs)}$ is the cross-PSD estimation of local signals and the GS. We divided the grey matter into 246 regions of interest (ROIs) defined by the Human Brainnetome Atlas and extracted the mean time course of each ROI to represent the ROI signal. This atlas was established by the FC method and has been demonstrated to show a better performance than several others in a clinical study (Lee et al., 2021). The number of FFT (NFFT) points was set to 512, while $P_{(roi,gs)}$ had a length of 257 calculated by (NFFT + 1)/2. Finally, a 246 × 257 C-matrix was obtained as the spatiotemporal GS topography for each subject.

The Pearson's correlation between age and each point of the C-matrix was calculated with gender as a covariate, obtaining a

246 × 257 matrix of GS-TV. The correlation coefficients were then converted to *Z* values using Fisher's *r*-to-*Z* transformation.

2.6 | Spatiotemporal dedifferentiation

Upon visual inspection, we observed an anticorrelation pattern between the GSCORR matrix and GS-TV. Specifically, higher GSCORR tended to get lower with age and vice versa, indicating a more homogeneous GSCORR distribution in the aging brain, that is, spatiotemporal dedifferentiation. To quantitatively assess this observation, we computed the Pearson's correlation between each pair of *C* and *Z*. The same operation was further performed across 246 regions and 257 frequency points to investigate the effect of spatial dedifferentiation and temporal dedifferentiation, respectively.

2.7 | Contributors detection for the spatiotemporal dedifferentiation

As suggested in previous studies, the GS is highly susceptible to vascular and physiological noises, which are significant variables in aging (Murphy & Fox, 2017; Power et al., 2017). To investigate these contributions, we incorporated three additional preprocessing protocols targeting head motion, white matter signals, cerebrospinal fluid signals, and neurovascular coupling effects. Detailed parameters for each protocol are outlined in Table 1.

A *Z*-test was subsequently conducted to compare these dedifferentiation maps with a dedifferentiation map derived from a classical preprocessing strategy, aiming to examine the influence of neurovascular and physiological noises. The methodologies applied in the third protocol are summarized briefly in the following section.

2.7.1 | Wavelet-despiking method for head motion

In our study, we calculated the coherence, which reflects the connectivity at each frequency point. This method is also recommended (Geerligs et al., 2017) to preprocess aging data. Thus, we applied this unsupervised approach to further reduce the influence of head motion over a range of frequencies. This technique identifies and eliminates abnormal events by detecting sequences of anomalous wavelet coefficients within the voxel time series. A significant metric employed in this method is the spike percentage. This serves as an indicator of the frequency at which corrections are made using the wavelet-despiking technique, representing the proportion of voxels within each data volume that encompass a spike. Evidently, this method is proficient in eliminating a wide range of motion artifacts, including the effects of spin-history and other high-frequency events. The original paper provides a comprehensive explanation of this approach (Patel et al., 2014).

2.7.2 | The component-based noise correction method

This approach employs the Principal Component Analysis to succinctly characterize the data derived from the signals of noise regions. Subsequently, principal components are integrated as covariates in a General Linear Model, serving as an approximation of the physiological noise signal space. In line with preceding studies, we executed a regression of the Component-based noise Correction method (CompCor) signals pertaining to both white matter and cerebrospinal fluid. This included their first-order derivatives, their square values, as well as their squared derivatives (Satterthwaite et al., 2013).

All of the cortical maps were visualized with the Connectome Workbench (Marcus et al., 2011). Subcortical maps were visualized with the DPABI package (http://www.restfmri.net) (Yan et al., 2016).

3 | RESULTS

3.1 | Spatiotemporal dedifferentiation of GS topography

The results obtained from the GSCORR matrix indicated higher values primarily in the posterior sensory cortices, which encompassed regions in the occipital, parietal, and temporal lobes, while the lowest values were observed in the association cortex (e.g., regions in the

TABLE 1 Different preprocessing strategies.

	Protocol 1 (main results, Figure 1)	Protocol 2 (without deconvolution, Figure 2)	Protocol 3 (strict control for physiological factors, Figure 3)	Protocol 4 (no control for physiological factors, Figure 3)
Wavelet-despiking	No	No	Yes	No
Classical regression	Yes	Yes	Yes	No
CompCor regression	No	No	Yes	No
Blind HRF deconvolution	Yes	No	Yes	Yes

Abbreviations: CompCor, component-based noise correction method; HRF, hemodynamic response function.

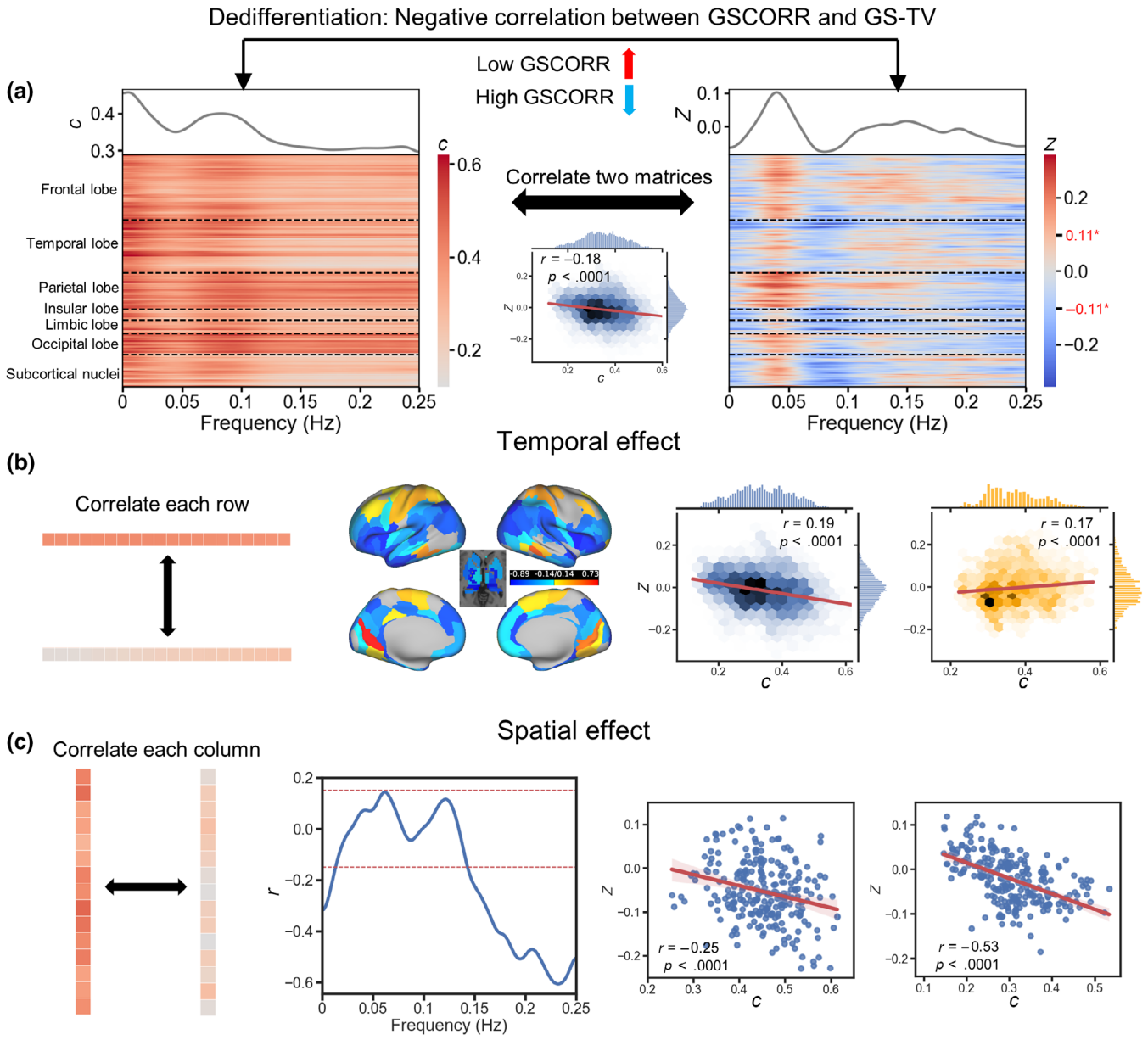

FIGURE 1 The spatiotemporal distribution of global signal (GS) topography and its spatiotemporal dedifferentiation with age. Panel (a), left: the grand averaged coherence between GS and local signals of all subjects (thermograph) and the mean coherence across all regions of interest (ROIs) (line chart). Right: correlations between GSCORR and age (thermograph) and the mean correlation coefficient across all ROIs (line chart). The red values with asterisks on the color bar indicate the threshold of significant *Z* values (FDR corrected, q < 0.05). Middle: the correlation between GSCORR and the variability of GS topography with age (GS-TV), that is, the overall spatiotemporal dedifferentiation of the GS topography with age. Panel (b): the temporal dedifferentiation of each ROI with dedifferentiated (negative) and differentiated (positive) tendencies. Panel (c): the spatial dedifferentiation (negative) of each frequency and the corresponding scatter charts of dedifferentiated bands. Red dotted lines represent the threshold of significant correlations (FDR corrected, $q < 0.05$). Significant *Z* value ($P < 0.05$, FDR corrected) are denoted with an asterisk (*).

frontal and temporal lobes belonging to the frontoparietal network and default mode network) and subcortical regions (Figure 1a). These findings were consistent with previous studies (Wang, Liao, et al., 2020; Yang et al., 2017; Zhang et al., 2020). The coherence curve showed a bi-peak distribution, which aligned with previous coherence studies (Drew et al., 2008; Li et al., 2015; Wang et al., 2016; Wang, Zou, et al., 2020). Meanwhile, the correlation between coherence and age showed a reverse trend (refer to line charts in Figures 1a and S1A). Specifically, GSCORRs showed higher values around ~0.02 and 0.06–0.1 Hz, but lower at 0.02–0.06 Hz and above 0.1 Hz, whereas GS-TVs displayed the opposite pattern. Overall, the GSCORR appeared to exhibit more homogeneity in the aging brain, as evidenced by the negative correlation between GS-TV and GSCORR (refer to Figures 1a and S1B).

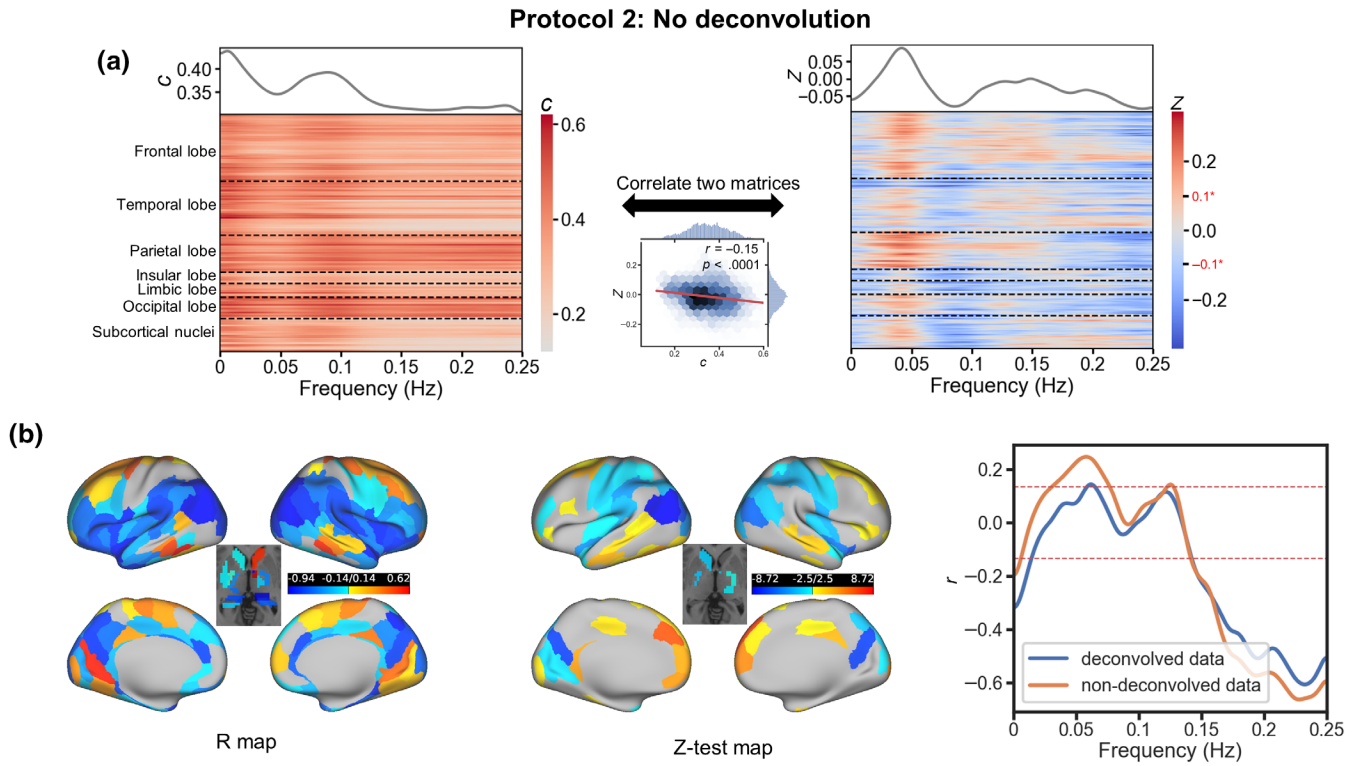

FIGURE 2 The spatiotemporal dedifferentiation and differentiation during brain aging in data without hemodynamic response function (HRF) de-convolution. Panel (a), GSCORR map, variability of global signal topography with age (GS-TV), and overall spatiotemporal dedifferentiation featured by the correlation between GSCORR and GS-TV. Panel (b), left: temporal dedifferentiation in each region of interest (ROI). Middle: difference between HRF deconvolved and no-deconvolved data for temporally dedifferentiation and differentiation in each ROI. Right: spatial dedifferentiation (negative) of each frequency. Red dotted lines represent the threshold of significant correlations (FDR corrected, $q < 0.05$). Significant Z value ($P < 0.05$, FDR corrected) are denoted with an asterisk (*).

As we observed an overall spatiotemporal dedifferentiation, we conducted further analysis to explore its characteristics in temporal and spatial dimensions, respectively. Considering the relatively small effect size of such dedifferentiation ($r^2 = 0.03$), we hypothesized the presence of certain differentiation effects. By averaging the temporal (row) and spatial (column) dimensions of the GSCORR and GS-TV, we detected small dedifferentiation effects in both time ($r^2 = 0.01$) and space ($r^2 = 0.03$). Our results, presented in Figures 1b and S1, indicated the temporal dedifferentiation in most brain regions with negative r values (FDR corrected, $q < 0.05$; see also Figure 1b, right), particularly in the association cortex. In contrast, the ventral visual pathway and sensorimotor regions exhibited a trend of temporal differentiation with positive r values (FDR corrected, $q < 0.05$; also refer to Figure 1b, right). Spatial dedifferentiation, as shown in Figures 1c and S1D, was found at approximately 0–0.014 and 0.143–0.25 Hz (see also Figure 1c, right). These findings suggest that spatiotemporal dedifferentiation dominates brain aging, although the sensorimotor system showed a trend of temporal differentiation.

3.2 | Minimal effects from neuro-vascular coupling

We also examined the GSCORR and GS-TV without HRF de-convolution and found consistent distributions with the HRF de-convolved data, as shown in Figure 2. The overall spatiotemporal dedifferentiation was replicated (Figure 2a, middle), and the temporal dedifferentiated and differentiated regions were similar to those in the HRF de-convolved data (Figure 2b, left), albeit with weakened trends in most regions, as indicated by reduced Z values in differentiated regions and increased Z values in dedifferentiated regions (Figure 2b, middle). The data without HRF de-convolution raised a trend of spatial differentiation at middle frequency (0.031–0.076 Hz) and remained spatial dedifferentiation at very low (0–0.005 Hz) and fast frequencies (0.141–0.25 Hz) (Figure 2b, right), although no significant difference between the two performances was found at any frequency points. These results suggest that neuro-vascular factors attenuated the trend of spatiotemporal dedifferentiation with age.

3.3 | Physiological factors attenuate age-related dedifferentiation

To ascertain the contribution of physiological factors, we applied two distinct preprocessing protocols. In protocol 3, which employed more stringent regression of these physiological factors, we observed a diminished effect of spatiotemporal dedifferentiation. Conversely, a more pronounced effect of spatiotemporal dedifferentiation was evident in the absence of noise regression (Figure 3a,c).

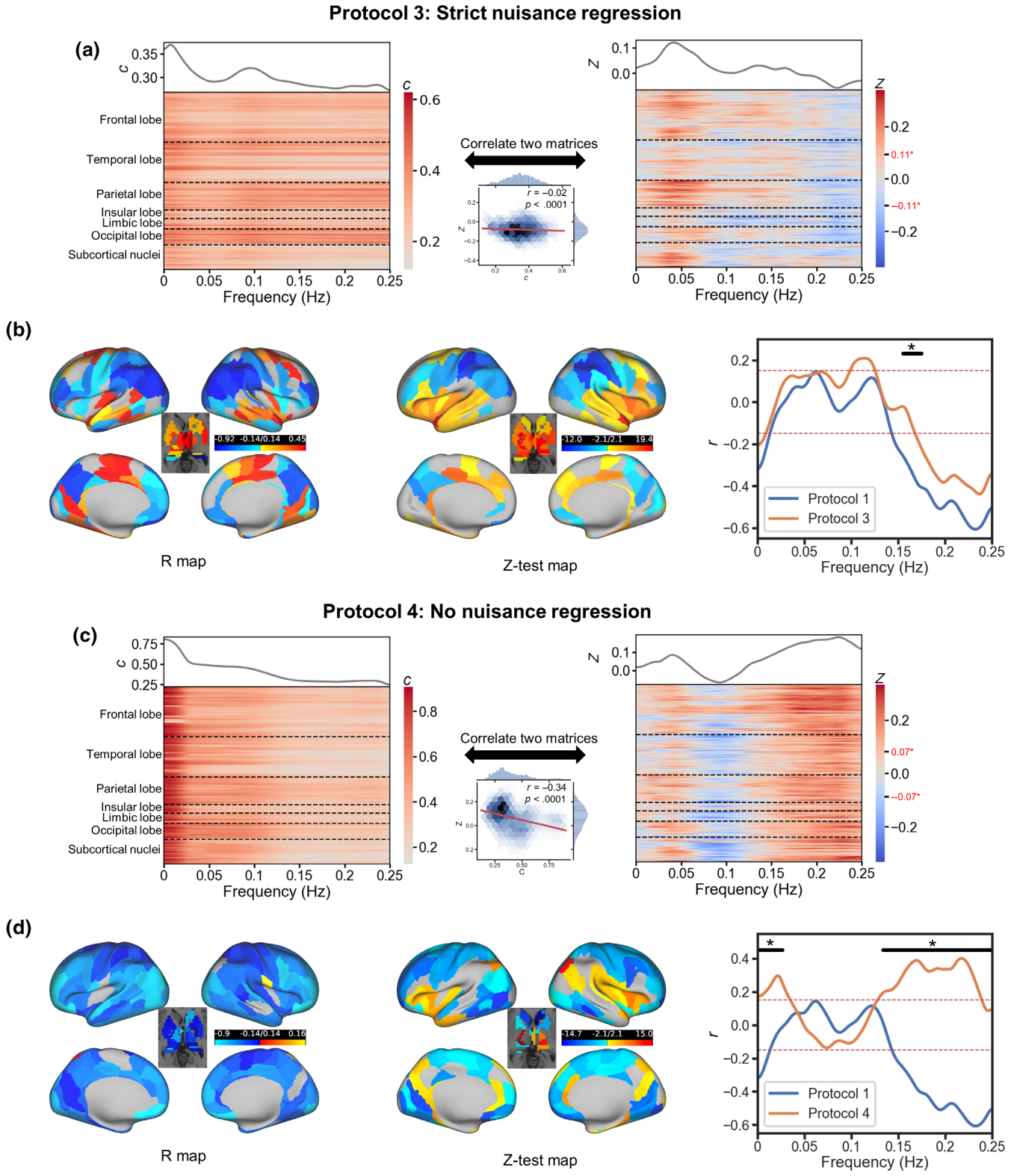

FIGURE 3 The spatiotemporal dedifferentiation and differentiation during brain aging in data with strict noise regression and without noise regression. Panels (a and c), GSCORR map, variability of global signal topography with age (GS-TV), and overall spatiotemporal dedifferentiation featured by the correlation between GSCORR and GS-TV. Panels (b and d), left: temporal dedifferentiation in each regions of interest (ROI). Middle: difference between hemodynamic response function deconvolved and no-deconvolved data for temporally dedifferentiation and differentiation in each ROI. Right: spatial dedifferentiation (negative) of each frequency. Red dotted lines represent the threshold of significant correlations (FDR corrected, $q < 0.05$). Significant Z value ($P < 0.05$, FDR corrected) are denoted with an asterisk (*).

The topographic distribution of temporal dedifferentiation effects largely remained consistent, indicating dedifferentiation in transmodal regions and differentiation in unimodal regions. However, the effect of spatial dedifferentiation was attenuated in protocol 3. In the absence of nuisance regression (protocol 4), temporal dedifferentiation was intensified. In terms of spatial effects, protocol 4 demonstrated trends opposite to those observed in protocol 1, with significantly different trends for spatial dedifferentiation and differentiation at 0–0.027 and 0.143–0.25 Hz, respectively. Significant spatial differentiation was observed at 0–0.035 and 0.127–0.239 Hz (Figure 3b,d).

In summary, the strongest spatiotemporal dedifferentiation was observed in the data without any nuisance control (protocol 4), with moderate dedifferentiation found in the data treated with classical preprocessing (protocol 1). Almost equal effects of dedifferentiation and differentiation were observed in the data subjected to highly rigorous nuisance control (protocol 3). Consequently, these results suggest that physiological factors such as head motion, white matter, and cerebrospinal fluid play substantial roles in causing age-related dedifferentiation.

4 | DISCUSSION

We investigated the spatiotemporal characteristics of GS topography and its age-related variations during resting-state, in order to provide a baseline for understanding the changes in GS topography in various cognitive tasks and mental disorders. Our findings showed that GS topography dynamically changed at the infra-slow frequency range below 0.25 Hz, as indicated by the bi-peak distribution of coherence, and across the lifespan from 18 to 80 years, as indicated by the age effect. More importantly, the GS topography exhibited an overall trend of spatiotemporal dedifferentiation with age, with dedifferentiation and differentiation tendencies present in both the temporal and spatial dimensions. These tendencies were attenuated by neural-vascular factors and reversed by physiological noises to some extent. To the best of our knowledge, this is the first study to extend the spatial dedifferentiation of brain aging to spatiotemporal dedifferentiation and to delineate dedifferentiation and differentiation at spatial and temporal dimensions, simultaneously.

4.1 | Spatiotemporal characteristics of GS topography and its age-related changes

We employed the coherence approach to estimate GS topography in spatial (i.e., brain region) and temporal (i.e., infra-slow frequency) dimensions. Coherence is a function of frequency indicating the correspondence of two power spectrum signals. Based on the Parseval's theorem, we have demonstrated that the PSD of the brain signal is equivalent to the brain signal variability (BSV) in the corresponding frequency band (Wang et al., 2018). BSV has been linked to the dynamic range of brain function and kinetic energy for the brain to achieve various potential states (Garrett et al., 2014). In this line, both PSD and BSV are considered to reflect the energy consumption of the brain (Wang et al., 2018). Thereby, the magnitude of coherence may reflect the consistency of energy consumption between ROIs in different time scales. Accordingly, the GSCORR reflects the consistency of energy consumption between local regions and the whole brain. The variation of GSCORR with age, in turn, may reflect age-related energy reallocation among functional subsystems and across time scales (Garrett et al., 2011; Wang et al., 2018).

We observed a bi-peak distribution of coherence coefficients, which is consistent with previous findings on coherence among local signals (Drew et al., 2008; Li et al., 2015; Sasai et al., 2014; Wang, Zou, et al., 2020). This finding suggests that BOLD signal fluctuations may complete particular brain functions through particular oscillating structures, in line with brain rhythms at traditional electroencephalogram (EEG) frequency ranges. Specifically, distinct GS topographies were captured at two peaks and two troughs of the coherence curve, supporting the "spectral fingerprints theory" that posits the frequency-specific coherence in large-scale functional networks as the "fingerprints" underlying cognitive processes (Siegel et al., 2012).

In line with the spectral fingerprint theory, we found that age-related variations of GS topography were frequency-specific. Although the psychological mechanisms of multiple low frequency bands remain unclear, many studies have focused on the frequency-specific effects of brain functions. For instance, the GS mainly affects the default mode network at 0.027–0.073 Hz, but also sensory regions at 0.01–0.027 Hz in patients with schizophrenia (Wang, Liao, et al., 2020). In addition, recent research by Wang and colleagues has demonstrated the frequency-dependent hub role of the dorsal and ventral anterior insula, highlighting that not only the spatial feature (i.e., dorsal and ventral regions) but also the temporal feature (i.e., multiple frequency bands) underlies compound psychological functions (Wang et al., 2018; Wang, Zou, et al., 2020). These studies suggested that specific psychological functions could be differentiated by different temporal scales of brain activity (Palva & Palva, 2018), supporting the spectral fingerprints theory (Siegel et al., 2012). Our findings provided new insight that age-related neural declines are captured by the GS topography in multiple low frequency bands. Overall, these results suggest that the neural functions associated with brain aging may depend on the specific spatiotemporal organization of the GS topography.

4.2 | The spatiotemporal dedifferentiation during brain aging

The dedifferentiation hypothesis and compensation hypothesis are two widely accepted theories of brain aging. The dedifferentiation hypothesis argues that the aging brain is accompanied by the loss of functional specificity in extensive brain regions engaged in various psychological functions (Natasha & Mark, 2005; Park et al., 2004). On the other hand, the compensation hypothesis posits that elders tend to recruit neural activity in brain regions involved in higher-order

cognitive functions to compensate for deficits in other regions (Wingfield & Grossman, 2006). The current results clearly show that the overall spatiotemporal structure of the GS topography becomes more homogeneous with age, supporting that the dedifferentiation is a primary mechanism of age-related variations of GS topography. This finding extends the dedifferentiation theory from the spatial dimension to the spatiotemporal matrix, suggesting that brain aging is accompanied by a homogeneous spatiotemporal structure.

In the temporal dimension, association regions exhibited the phenomenon of dedifferentiation, whereas some sensory and motor regions showed a tendency of differentiation. The different trends of aging in unimodal and multimodal regions are consistent with the intrinsic organization of GS topography (Ao et al., 2021; Yang et al., 2017) as well as large-scale gradients in cortical organization of the human brain (Huntenburg et al., 2018). Both GS topography and cortical gradients have been demonstrated to correspond well with the principal spatial gene expression pattern, the cortical myelination pattern, and the cortical excitation/inhibition balance (Brown et al., 2022), suggesting the dedifferentiation in multimodal regions and differentiation in sensorimotor regions to be supported by the biological evolution with age.

Several recent studies have highlighted the age-related sensory-association segregation in dedifferentiation and differentiation of aging. For instance, Grady and colleagues found that most brain regions showed less BSV with older age whereas a few regions (e.g., the superior frontal gyrus and some subcortical regions) showed increased BSV with age (Grady & Garrett, 2014). In a combined fMRI-EEG study, Kumral and colleagues found that variabilities of BOLD and EEG signals in most frequency bands and brain regions are consistently decreased with aging, but the temporal and sensorimotor regions show an age-related increase of variability of beta EEG oscillations (Kumral et al., 2020). Using longitudinal aging data, Malagurski et al. (2020) found an age-related decrease of segregation indices in most brain networks but an increase in the limbic network. These findings, combined with ours, suggest that dedifferentiation and differentiation in aging coexist but in different brain regions. However, only the variation of GS topography with age mirrored the intrinsic gradient organization of brain functions.

The spatial dedifferentiation was mainly restricted at the lower and higher ends of the frequency range, suggesting that spatial dedifferentiation is constrained by time scales. However, the spatial dedifferentiation was located at 0–0.014 and 0.143–0.25 Hz, which is inconsistent with previous findings that spatial dedifferentiation occurs in the intermediate frequencies (often at 0.01–0.1 Hz) (Chan et al., 2014; Malagurski et al., 2020). Previous studies often examined spatial dedifferentiation with activation, inter-regional FC, or graph theory, while abundant evidence has revealed that GS regression alters resting-state FC within and between networks, suggesting that the GS itself contains variability of global connectivity (Scalabrini et al., 2020). Different from GS affecting local activity in higher frequency bands, local activity mainly affects GS at the lowest frequency end (Wang et al., 2023), indicating that the spatial dedifferentiation may be driven by various interactions between GS and local signals at different time scales. Considering that neural oscillations at lower frequencies are associated with functions of larger neural networks and higher-order cognition (Buzsáki, 2006), spatial dedifferentiation at the higher frequency end may be driven by more homogeneous local activities while at the lower frequency end may primarily be driven by the GS. This hypothesis warrants further investigation.

4.3 | Assessment of physiological "noise"

There is abundant nonneural information in the GS and local BOLD signals that impacts neural activities in complex ways (Birn, 2012; Boubela et al., 2013). Therefore, we tested the influence of HRF de-convolution and noise regression on the current findings.

We found that spatiotemporal dedifferentiation was slightly weakened in data that did not undergo HRF de-convolution, which was mainly manifested as weakened temporal dedifferentiation in most brain regions. Furthermore, we observed significant spatial differentiation within 0.031–0.076 Hz. These findings suggest that neurovascular factors tend to preserve the pattern of spatiotemporal differentiation in the elderly brain. Although some studies found unchanged neurovascular coupling with normal aging (D'Esposito et al., 1999; Grinband et al., 2017), others have suggested that neurovascular, cardiovascular, and cerebrovascular factors could explain brain aging to a large extent (Fabiani et al., 2014; Tsvetanov et al., 2021). A large number of studies have revealed that cerebral hemodynamic activities at 0.04–0.1 Hz reflect underlying neural information (Auer, 2008; Du et al., 2014; Fox & Raichle, 2007; Ma et al., 2016; Tong & Frederick, 2010; Wright et al., 2017; Xie et al., 2016). Yang et al. (2018) also revealed cognitive-related frequency and amplitude modulation in aging at 0.045–0.087 Hz, suggesting that neurovascular factors at this frequency band are cognitive-related. Although the blind de-convolution algorithm cannot fully remove vascular effects, it was shown that neurovascular coupling could be an important protective factor of aging to some extent.

Traditional physiological noises including head motion, white matter, and cerebrospinal fluid signals, strengthened spatiotemporal dedifferentiation in general. However, they preserved spatial differentiation perhaps at the expense of increasing temporal dedifferentiation. The migration of brain signal fluctuations from lower frequencies to higher frequencies was observed during both lifespan development and cognitive tasks (Churchill et al., 2016; He, 2011), resulting in the weakening of scale-free properties and enhancement of temporal dedifferentiation. This temporal reorganization of brain activities was suggested to reflect the brain engaging with more effort on immediate functional networks (He et al., 2010). Although the temporal dedifferentiation of aging has been uncovered (Ao et al., 2022) and verified here, it is still unknown how these altered temporal structures influence and interact with the spatial organization of brain function during brain aging. Therefore, the spatiotemporal perspective is valuable for uncovering the dynamic organization of brain functions across temporal and spatial dimensions.

In addition, the HRF de-convolution and noise regression exerted distinct effects on different frequencies and regions, suggesting that neural, physiological, and other signals have separable spatiotemporal structures. Considering that physiological networks nicely mirrored neural networks (Chen et al., 2020), the opposite trend of spatial dedifferentiation between data with and without noise regression suggested that GS topography may serve as an alternative approach to separate neural signals and physiological noises. On the other side, head motion (Zeng et al., 2014), white matter (Li et al., 2019), cerebrospinal fluid (Fultz et al., 2019), respiratory (Park et al., 2020), and cardiac signals (Mosher et al., 2020) have been demonstrated to contain meaningful physiological and pathological information. This evidence argues that noise plays an important role in brain function (Ghosh et al., 2008; McDonnell & Ward, 2011; Mišić et al., 2010).

Our results demonstrated that the GS topography holds a strong promise to reveal the changes of age-related brain functions. Our findings suggested that it is critical for future studies to pay caution to "noises" when interpreting their results. As Uddin has argued, "as we continue to embrace the idea that there may be untapped information in spontaneous neural activity, perhaps we should not be so hasty in future efforts to separate brain signal from noise" (Uddin, 2020).

4.4 | Limitations

Several limitations should be taken into account in our study. First, the precise sources of the age-related dedifferentiation observed here cannot be determined with certainty as the physiological data such as respiratory and cardiac signals were not available in the dataset. While we re-analyzed the data without HRF de-convolution and nuisance regression, future studies should consider collecting simultaneous physiological recordings, given the complex interplay between neural and vascular activities (Das et al., 2021). Moreover, our study did not account for the nonzero lag effects of neurovascular coupling, white matter, and cerebrospinal fluid, which calls for future research on brain aging.

Secondly, the subjects were not uniformly distributed in age (Wei et al., 2018), which may have influenced the correlation between age and GS topography to some extent. Finally, it is important to note that the dedifferentiation theory of aging is primarily associated with cognitive performance. As our study only examined the phenomenon of spontaneous brain activities without cognitive tasks, the findings should be interpreted with caution.

5 | CONCLUSION

The GS topography has an intrinsic spatiotemporal architecture and varies with age. Brain aging exhibits spatial and temporal dimensions which are characterized by distinct dedifferentiation and differentiation trends, originating from different signals or "noises." Our discovery of the spatiotemporal dedifferentiation phenomenon provides novel insights into the spatiotemporal organizational mechanisms underlying brain aging. These findings serve as a catalyst for future research, enabling more nuanced examinations of age-related functional connectivity at both the global and local levels.

ACKNOWLEDGEMENTS

This research has received funding from National Natural Science Foundation of China (62177035). Y.A. is grateful for the support from China Scholarship Council (202208510069). We are grateful for the time and effort devoted by editors and anonymous reviewers to improving the quality of published work.

CONFLICT OF INTEREST STATEMENT

The authors declare that the research was conducted in the absence of any commercial or financial relationships that could be construed as a potential conflict of interest.

DATA AVAILABILITY STATEMENT

The MRI datasets used in this study are available to the public from the International Data-sharing Initiative (http://fcon_1000.projects.nitrc.org/indi/retro/sald.html). All the availabilities of software and code used in the study are stated in Section 2.

ORCID

Yifeng Wang https://orcid.org/0000-0002-0743-9986

REFERENCES

Adaikkan, C., Middleton, S. J., Marco, A., Pao, P. C., Mathys, H., Kim, D. N. W., Gao, F., Young, J. Z., Suk, H. J., Boyden, E. S., McHugh, T. J., & Tsai, L. H. (2019). Gamma entrainment binds higher-order brain regions and offers neuroprotection. *Neuron*, *102*(5), 929–943.

Ao, Y., Kou, J., Yang, C., Wang, Y., Huang, L., Jing, X., Cui, Q., Cai, X., & Chen, J. (2022). The temporal dedifferentiation of global brain signal fluctuations during human brain ageing. *Scientific Reports*, *12*(1), 3616. https://doi.org/10.1038/s41598-022-07578-6

Ao, Y., Ouyang, Y., Yang, C., & Wang, Y. (2021). Global signal topography of the human brain: A novel framework of functional connectivity for psychological and pathological investigations. *Frontiers in Human Neuroscience*, *15*, 644892. https://doi.org/10.3389/fnhum.2021.644892

Auer, D. P. (2008). Spontaneous low-frequency blood oxygenation level-dependent fluctuations and functional connectivity analysis of the 'resting' brain. *Journal of Magnetic Resonance Imaging*, *26*(7), 1055–1064. https://doi.org/10.1016/j.mri.2008.05.008

Baltes, P. B., & Lindenberger, U. (1997). Emergence of a powerful connection between sensory and cognitive functions across the adult life span: A new window to the study of cognitive aging? *Psychology and Aging*, *12*(1), 12–21.

Baria, A. T., Baliki, M. N., Parrish, T., & Apkarian, A. V. (2011). Anatomical and functional assemblies of brain BOLD oscillations. *Journal of Neuroscience*, *31*(21), 7910–7919.

Birn, R. M. (2012). The role of physiological noise in resting-state functional connectivity. *NeuroImage*, *62*(2), 864–870.

Boubela, R. N., Kalcher, K., Huf, W., Kronnerwetter, C., Filzmoser, P., & Moser, E. (2013). Beyond noise: Using temporal ICA to extract meaningful information from high-frequency fMRI signal fluctuations during rest. *Frontiers in Human Neuroscience*, *7*, 1–12.

Brown, J. A., Lee, A. J., Pasquini, L., & Seeley, W. W. (2022). A dynamic gradient architecture generates brain activity states. *NeuroImage*, *261*, 119526.

Buzsáki, G. (2006). *Rhythms of the brain*. Oxford University Press.

Buzsáki, G., & Draguhn, A. (2004). Neuronal oscillations in cortical networks. *Science*, *304*(5679), 1926–1929.

Cao, M., Wang, J., Dai, Z., Cao, X., Jiang, L., Fan, F., Song, X., Xia, M., Shu, N., Dong, Q., Milham, M. P., Xavier Castellanos, F., Zuo, X., He, Y., & He, Y. (2014). Topological organization of the human brain functional connectome across the lifespan. *Developmental Cognitive Neuroscience*, *7*(1), 76–93.

Chan, M. Y., Park, D. C., Savalia, N. K., Petersen, S. E., & Wig, G. S. (2014). Decreased segregation of brain systems across the healthy adult lifespan. *Proceedings of the National Academy of Sciences of the United States of America*, *111*(46), E4997–E5006. https://doi.org/10.1073/pnas.1415122111

Chen, H., Duan, X., Liu, F., Lu, F., Ma, X., Zhang, Y., Uddin, L. Q., & Chen, H. (2016). Multivariate classification of autism spectrum disorder using frequency-specific resting-state functional connectivity – A multi-center study. *Progress in Neuro-Psychopharmacology and Biological Psychiatry*, *64*, 1–9.

Chen, J. E., Lewis, L. D., Chang, C., Tian, Q., Fultz, N. E., Ohringer, N. A., Rosen, B. R., & Polimeni, J. R. (2020). Resting-state "physiological networks". *NeuroImage*, *213*, 116707.

Churchill, N. W., Spring, R., Grady, C., Cimprich, B., Askren, M. K., Reuter-Lorenz, P. A., Jung, M. S., Peltier, S., Strother, S. C., & Berman, M. G. (2016). The suppression of scale-free fMRI brain dynamics across three different sources of effort: Aging, task novelty and task difficulty. *Scientific Reports*, *6*, 30895.

Damoiseaux, J. S. (2017). Effects of aging on functional and structural brain connectivity. *NeuroImage*, *160*, 32–40. https://doi.org/10.1016/j.neuroimage.2017.01.077

Das, A., Murphy, K., & Drew, P. J. (2021). Rude mechanicals in brain haemodynamics: Non-neural actors that influence blood flow. *Philosophical Transactions of the Royal Society of London. Series B, Biological Sciences*, *376*(1815), 20190635. https://doi.org/10.1098/rstb.2019.0635

De Domenico, M., Sasai, S., & Arenas, A. (2016). Mapping multiplex hubs in human functional brain networks. *Frontiers in Neuroscience*, *10*, 326. https://doi.org/10.3389/fnins.2016.00326

D'Esposito, M., Zarahn, E., Aguirre, G. K., & Rypma, B. (1999). The effect of normal aging on the coupling of neural activity to the bold hemodynamic response. *NeuroImage*, *10*(1), 6–14.

Drew, P. J., Duyn, J. H., Golanov, E., & Kleinfeld, D. (2008). Finding coherence in spontaneous oscillations. *Nature Neuroscience*, *11*(9), 991–993.

Du, C., Volkow, N. D., Koretsky, A. P., & Pan, Y. (2014). Low-frequency calcium oscillations accompany deoxyhemoglobin oscillations in rat somatosensory cortex. *Proceedings of the National Academy of Sciences of the United States of America*, *111*(43), E4677–E4686. https://doi.org/10.1073/pnas.1410800111

Fabiani, M., Gordon, B. A., Maclin, E. L., Pearson, M. A., Brumback-Peltz, C. R., Low, K. A., McAuley, E., Sutton, B. P., Kramer, A. F., & Gratton, G. (2014). Neurovascular coupling in normal aging: A combined optical, ERP and fMRI study. *NeuroImage*, *85*, 592–607.

Fan, L., Li, H., Zhuo, J., Zhang, Y., Wang, J., Chen, L., Yang, Z., Chu, C., Xie, S., Laird, A. R., Fox, P. T., Eickhoff, S. B., Yu, C., & Jiang, T. (2016). The human brainnetome atlas: A new brain atlas based on connectional architecture. *Cerebral Cortex*, *26*(8), 3508–3526. https://doi.org/10.1093/cercor/bhw157

Ferreira, L. K., & Busatto, G. F. (2013). Resting-state functional connectivity in normal brain aging. *Neuroscience and Biobehavioral Reviews*, *37*, 384–400.

Fiebelkorn, I. C., & Kastner, S. (2019). A rhythmic theory of attention. *Trends in Cognitive Sciences*, *23*(2), 87–101. https://doi.org/10.1016/j.tics.2018.11.009

Fox, M. D., & Raichle, M. E. (2007). Spontaneous fluctuations in brain activity observed with functional magnetic resonance imaging. *Nature Review Neuroscience*, *8*(9), 700–711. https://doi.org/10.1038/nrn2201

Fox, M. D., Snyder, A. Z., Vincent, J. L., Corbetta, M., Van Essen, D. C., & Raichle, M. E. (2005). The human brain is intrinsically organized into dynamic, anticorrelated functional networks. *Proceedings of the National Academy of Sciences of the United States of America*, *102*(27), 9673–9678.

Fox, M. D., Zhang, D., Snyder, A. Z., & Raichle, M. E. (2009). The global signal and observed anticorrelated resting state brain networks. *Journal of Neurophysiology*, *101*(6), 3270–3283. https://doi.org/10.1152/jn.90777.2008

Fultz, N. E., Bonmassar, G., Setsompop, K., Stickgold, R. A., Rosen, B. R., Polimeni, J. R., & Lewis, L. D. (2019). Coupled electrophysiological, hemodynamic, and cerebrospinal fluid oscillations in human sleep. *Science*, *366*, 628–631.

Garrett, D. D., Kovacevic, N., McIntosh, A. R., & Grady, C. L. (2011). The importance of being variable. *Journal of Neuroscience*, *31*(12), 4496–4503. https://doi.org/10.1523/JNEUROSCI.5641-10.2011

Garrett, D. D., McIntosh, A. R., & Grady, C. L. (2014). Brain signal variability is parametrically modifiable. *Cerebral Cortex*, *24*(11), 2931–2940. https://doi.org/10.1093/cercor/bht150

Geerligs, L., Tsvetanov, K. A., & Henson, R. N. (2017). Challenges in measuring individual differences in functional connectivity using fMRI: The case of healthy aging. *Human Brain Mapping*, *38*(8), 4125–4156.

Ghosh, A., Rho, Y., McIntosh, A. R., Kötter, R., & Jirsa, V. K. (2008). Noise during rest enables the exploration of the brain's dynamic repertoire. *PLoS Computational Biology*, *4*(10), e1000196.

Grady, C. L., & Garrett, D. D. (2014). Understanding variability in the BOLD signal and why it matters for aging. *Brain Imaging and Behavior*, *8*, 274–283.

Grinband, J., Steffener, J., Razlighi, Q. R., & Stern, Y. (2017). BOLD neurovascular coupling does not change significantly with normal aging. *Human Brain Mapping*, *38*(7), 3538–3551.

Han, S., Zong, X., Hu, M., Yu, Y., Wang, X., Long, Z., Wang, Y., Chen, X., & Chen, H. (2017). Frequency-selective alteration in the resting-state corticostriatal-thalamo-cortical circuit correlates with symptoms severity in first-episode drug-naive patients with schizophrenia. *Schizophrenia Research*, *189*, 175–180.

He, B. J. (2011). Scale-free properties of the functional magnetic resonance imaging signal during rest and task. *Journal of Neuroscience*, *31*(39), 13786–13795.

He, B. J., Zempel, J. M., Snyder, A. Z., & Raichle, M. E. (2010). The temporal structures and functional significance of scale-free brain activity. *Neuron*, *66*(3), 353–369.

Huntenburg, J. M., Bazin, P. L., & Margulies, D. S. (2018). Large-scale gradients in human cortical organization. *Trends in Cognitive Sciences*, *22*(1), 21–31. https://doi.org/10.1016/j.tics.2017.11.002

Jenkinson, M., Bannister, P., Brady, M., & Smith, S. (2002). Improved optimization for the robust and accurate linear registration and motion correction of brain images. *NeuroImage*, *17*(2), 825–841. https://doi.org/10.1016/s1053-8119(02)91132-8

Koen, J. D., & Rugg, M. D. (2019). Neural dedifferentiation in the aging brain. *Trends in Cognitive Sciences*, *23*(7), 547–559. https://doi.org/10.1016/j.tics.2019.04.012

Koen, J. D., Srokova, S., & Rugg, M. D. (2020). Age-related neural dedifferentiation and cognition. *Current Opinion in Behavioral Sciences*, *32*, 7–14. https://doi.org/10.1016/j.cobeha.2020.01.006

Krishnan, G. P., González, O. C., & Bazhenov, M. (2018). Origin of slow spontaneous resting-state neuronal fluctuations in brain networks. *Proceedings of the National Academy of Sciences of the United States of America*, *115*(26), 6858–6863.

Kumral, D., Şansal, F., Cesnaite, E., Mahjoory, K., Al, E., Gaebler, M., Nikulin, V. V., & Villringer, A. (2020). BOLD and EEG signal variability at rest differently relate to aging in the human brain. *Neuroimage*, *207*, 116373. https://doi.org/10.1016/j.neuroimage.2019.116373

Lee, J. J., Kim, H. J., Ceko, M., Park, B. Y., Lee, S. A., Park, H., Roy, M., Kim, S. G., Wager, T. D., & Woo, C. W. (2021). A neuroimaging

biomarker for sustained experimental and clinical pain. *Nature Medicine*, *27*(1), 174–182. https://doi.org/10.1038/s41591-020-1142-7

Li, J. M., Bentley, W. J., Snyder, A. Z., Raichle, M. E., & Snyder, L. H. (2015). Functional connectivity arises from a slow rhythmic mechanism. *Proceedings of the National Academy of Sciences of the United States of America*, *112*(19), E2527–E2535. https://doi.org/10.1073/pnas.1419837112

Li, M., Newton, A. T., Anderson, A. W., Ding, Z., & Gore, J. C. (2019). Characterization of the hemodynamic response function in white matter tracts for event-related fMRI. *Nature Communications*, *10*, 1140.

Lou, W., Wang, D., Wong, A., Chu, W. C. W., Mok, V. C. T., & Shi, L. (2019). Frequency-specific age-related decreased brain network diversity in cognitively healthy elderly: A whole-brain datadriven analysis. *Human Brain Mapping*, *40*, 340–351.

Ma, Y., Shaik, M. A., Kozberg, M. G., Kim, S. H., Portes, J. P., Timerman, D., & Hillman, E. M. (2016). Resting-state hemodynamics are spatiotemporally coupled to synchronized and symmetric neural activity in excitatory neurons. *Proceedings of the National Academy of Sciences of the United States of America*, *113*(52), E8463–E8471. https://doi.org/10.1073/pnas.1525369113

Malagurski, B., Liem, F., Oschwald, J., Merillat, S., & Jancke, L. (2020). Functional dedifferentiation of associative resting state networks in older adults – A longitudinal study. *NeuroImage*, *214*, 116680. https://doi.org/10.1016/j.neuroimage.2020.116680

Marcus, D. S., Harwell, J., Olsen, T., Hodge, M., Glasser, M. F., Prior, F., Jenkinson, M., Laumann, T., Curtiss, S. W., & Van Essen, D. C. (2011). Informatics and data mining tools and strategies for the human connectome project. *Frontiers in Neuroinformatics*, *5*, 4. https://doi.org/10.3389/fninf.2011.00004

McDonnell, M. D., & Ward, L. M. (2011). The benefits of noise in neural systems: Bridging theory and experiment. *Nature Reviews Neuroscience*, *12*(7), 415–426.

Mišić, B., Mills, T., Taylor, M. J., & McIntosh, A. R. (2010). Brain noise is task dependent and region specific. *Journal of Neurophysiology*, *104*(5), 2667–2676.

Mosher, C. P., Wei, Y., Kamiński, J., Nandi, A., Mamelak, A. N., Anastassiou, C. A., & Rutishauser, U. (2020). Cellular classes in the human brain revealed in vivo by heartbeat-related modulation of the extracellular action potential waveform. *Cell Reports*, *30*(10), 3536–3551.

Murphy, K., & Fox, M. D. (2017). Towards a consensus regarding global signal regression for resting state functional connectivity MRI. *NeuroImage*, *154*, 169–173.

Natasha, R. M., & Mark, D. E. (2005). Region-specific changes in prefrontal function with age: A review of PET and fMRI studies on working and episodic memory. *Brain*, *128*(9), 1964–1983.

Palva, S., & Palva, J. M. (2018). Roles of brain criticality and multiscale oscillations in temporal predictions for sensorimotor processing. *Trends in Neurosciences*, *41*(10), 729–743.

Park, D. C., Polk, T. A., Park, R., Minear, M., Savage, A., & Smith, M. R. (2004). Aging reduces neural specialization in ventral visual cortex. *Proceedings of the National Academy of Sciences of the United States of America*, *101*(35), 13091–13095. https://doi.org/10.1073/pnas.0405148101

Park, H.-D., Barnoud, C., Trang, H., Kannape, O. A., Schaller, K., & Blanke, O. (2020). Breathing is coupled with voluntary action and the cortical readiness potential. *Nature Communications*, *11*, 289.

Patel, A. X., Kundu, P., Rubinov, M., Jones, P. S., Vértes, P. E., Ersche, K. D., Suckling, J., & Bullmore, E. T. (2014). A wavelet method for modeling and despiking motion artifacts from resting-state fMRI time series. *NeuroImage*, *95*, 287–304.

Perrault, A. A., Khani, A., Quairiaux, C., Kompotis, K., Franken, P., Muhlethaler, M., Schwartz, S., & Bayer, L. (2019). Whole-night continuous rocking entrains spontaneous neural oscillations with benefits for sleep and memory. *Current Biology*, *29*(3), 402–411.

Power, J. D. (2019). Temporal ICA has not properly separated global fMRI signals: A comment on Glasser et al. (2018). *Neuroimage*, *197*, 650–651.

Power, J. D., Mitra, A., Laumann, T. O., Snyder, A. Z., Schlaggar, B. L., & Petersen, S. E. (2014). Methods to detect, characterize, and remove motion artifact in resting state fMRI. *NeuroImage*, *84*, 320–341.

Power, J. D., Plitt, M., Laumann, T. O., & Martin, A. (2017). Sources and implications of whole-brain fMRI signals in humans. *NeuroImage*, *146*, 609–625.

Sala-Llonch, R., Bartrés-Faz, D., & Junque, C. (2015). Reorganization of brain networks in aging: A review of functional connectivity studies. *Frontiers in Psychology*, *6*, 663.

Salvador, R., Martinez, A., Pomarol-Clotet, E., Gomar, J., Vila, F., Sarro, S., Capdevila, A., & Bullmore, E. (2008). A simple view of the brain through a frequency-specific functional connectivity measure. *NeuroImage*, *39*(1), 279–289.

Sasai, S., Homae, F., Watanabe, H., Sasaki, A. T., Tanabe, H. C., Sadato, N., & Taga, G. (2014). Frequency-specific network topologies in the resting human brain. *Frontiers in Human Neuroscience*, *8*, 1–19.

Sasai, S., Koike, T., Sugawara, S. K., Hamano, Y. H., Sumiya, M., Okazaki, S., Takahashi, H. K., Taga, G., & Sadato, N. (2021). Frequency-specific task modulation of human brain functional networks: A fast fMRI study. *NeuroImage*, *224*, 117375. https://doi.org/10.1016/j.neuroimage.2020.117375

Satterthwaite, T. D., Elliott, M. A., Gerraty, R. T., Ruparel, K., Loughead, J., Calkins, M. E., Eickhoff, S. B., Hakonarson, H., Gur, R. C., Gur, R. E., & Wolf, D. H. (2013). An improved framework for confound regression and filtering for control of motion artifact in the preprocessing of resting-state functional connectivity data. *NeuroImage*, *64*, 240–256.

Scalabrini, A., Vai, B., Poletti, S., Damiani, S., Mucci, C., Colombo, C., Zanardi, R., Benedetti, F., & Northoff, G. (2020). All roads lead to the default-mode network-global source of DMN abnormalities in major depressive disorder. *Neuropsychopharmacology*, *45*(12), 2058–2069. https://doi.org/10.1038/s41386-020-0785-x

Schölvinck, M. L., Maier, A., Frank, Q. Y., Duyn, J. H., & Leopold, D. A. (2010). Neural basis of global resting-state fMRI activity. *Proceedings of the National Academy of Sciences of the United States of America*, *107*(22), 10238–10243.

Siegel, M., Donner, T. H., & Engel, A. K. (2012). Spectral fingerprints of large-scale neuronal interactions. *Nature Review Neuroscience*, *13*(2), 121–134. https://doi.org/10.1038/nrn3137

Tanabe, S., Huang, Z., Zhang, J., Chen, Y., Fogel, S., Doyon, J., Wu, J., Xu, J., Zhang, J., Qin, P., Wu, X., Mao, Y., Mashour, G. A., Hudetz, A. G., & Northoff, G. (2020). Altered global brain signal during physiologic, pharmacologic, and pathologic states of unconsciousness in humans and rats. *Anesthesiology*, *132*(6), 1392–1406. https://doi.org/10.1097/ALN.0000000000003197

Tarantini, S., Tran, C. H. T., Gordon, G. R., Ungvari, Z., & Csiszar, A. (2017). Impaired neurovascular coupling in aging and Alzheimer's disease: Contribution of astrocyte dysfunction and endothelial impairment to cognitive decline. *Experimental Gerontology*, *94*, 52–58.

Tian, L., Li, Q., Wang, C., & Yu, J. (2018). Changes in dynamic functional connections with aging. *NeuroImage*, *172*, 31–39.

Tomasi, D., & Volkow, N. D. (2012). Aging and functional brain networks. *Molecular Psychiatry*, *17*(5), 549–558.

Tong, Y., & Frederick, B. D. (2010). Time lag dependent multimodal processing of concurrent fMRI and near-infrared spectroscopy (NIRS) data suggests a global circulatory origin for low-frequency oscillation signals in human brain. *NeuroImage*, *53*(2), 553–564. https://doi.org/10.1016/j.neuroimage.2010.06.049

Tsvetanov, K. A., Henson, R. N. A., Jones, P. S., Mutsaerts, H., Fuhrmann, D., Tyler, L. K., Cam-CAN, & Rowe, J. B. (2021). The effects of age on resting-state BOLD signal variability is explained by cardiovascular and cerebrovascular factors. *Psychophysiology*, *58*, e13714.

Uddin, L. Q. (2020). Bring the noise: Reconceptualizing spontaneous neural activity. *Trends in Cognitive Sciences*, *24*(9), 734–746. https://doi.org/10.1016/j.tics.2020.06.003

Vij, S. G., Nomi, J. S., Dajania, D. R., & Uddin, L. Q. (2018). Evolution of spatial and temporal features of functional brain networks across the lifespan. *NeuroImage*, *173*, 498–508.

Wang, X., Liao, W., Han, S., Li, J., Wang, Y., Zhang, Y., Zhao, J., & Chen, H. (2020). Frequency-specific altered global signal topography in drug-naive first-episode patients with adolescent-onset schizophrenia. *Brain Imaging and Behavior*, *15*, 1876–1885. https://doi.org/10.1007/s11682-020-00381-9

Wang, X., Liao, W., Han, S., Li, J., Zhang, Y., Zhao, J., & Chen, H. (2019). Altered dynamic global signal topography in antipsychotic-naive adolescents with early-onset schizophrenia. *Schizophrenia Research*, *208*, 308–316. https://doi.org/10.1016/j.schres.2019.01.035

Wang, Y., Chen, W., Ye, L., Biswal, B. B., Yang, X., Zou, Q., Yang, P., Yang, Q., Wang, X., Cui, Q., Duan, X., Liao, W., & Chen, H. (2018). Multiscale energy reallocation during low-frequency steady-state brain response. *Human Brain Mapping*, *39*, 2121–2132.

Wang, Y., Huang, X., Yang, X., Yang, Q., Wang, X., Northoff, G., Pang, Y., Wang, C., Cui, Q., & Chen, H. (2019). Low-frequency phase-locking of brain signals contribute to efficient face recognition. *Neuroscience*, *422*, 172–183.

Wang, Y., Liu, F., Long, Z.-L., Duan, X.-J., Cui, Q., Yan, J. H., & Chen, H.-F. (2014). Steady-state BOLD response modulates low frequency neural oscillations. *Scientific Reports*, *4*, 7376.

Wang, Y., Long, Z., Cui, Q., Liu, F., Jing, X. J., Chen, H., Guo, X. N., Yan, J. H., Chen, H. F., & Chen, H. F. (2016). Low frequency steady-state brain responses modulate large scale functional networks in a frequency-specific means. *Human Brain Mapping*, *37*, 381–394.

Wang, Y., Wang, X., Ye, L., Yang, Q., Cui, Q., He, Z., Li, L., Yang, X., Zou, Q., Yang, P., Liu, D., & Chen, H. (2019). Spatial complexity of brain signal is altered in patients with generalized anxiety disorder. *Journal of Affective Disorders*, *246*, 387–393.

Wang, Y., Yang, C., Li, G., Ao, Y., Jiang, M., Cui, Q., Pang, Y., & Jing, X. (2023). Frequency-dependent effective connections between local signals and the global brain signal during resting-state. *Cognitive Neurodynamics*, *17*, 555–560. https://doi.org/10.1007/s11571-11022-09831-11570

Wang, Y., Zou, Q., Ao, Y., Liu, Y., Ouyang, Y., Wang, X., Biswal, B., Cui, Q., & Chen, H. (2020). Frequency-dependent circuits anchored in the dorsal and ventral left anterior insula. *Scientific Reports*, *10*(1), 16394. https://doi.org/10.1038/s41598-020-73192-z

Wang, Y.-F., Dai, G.-S., Liu, F., Long, Z.-L., Yan, J. H., & Chen, H.-F. (2015). Steady-state BOLD response to higher-order cognition modulates low frequency neural oscillations. *Journal of Cognitive Neuroscience*, *27*(12), 2406–2415.

Watrous, A. J., Tandon, N., Conner, C. R., Pieters, T., & Ekstrom, A. D. (2013). Frequency-specific network connectivity increases underlie accurate spatiotemporal memory retrieval. *Nature Neuroscience*, *16*(3), 349–356.

Wei, D., Zhuang, K., Ai, L., Chen, Q., Yang, W., Liu, W., Wang, K., Sun, J., & Qiu, J. (2018). Structural and functional brain scans from the cross-sectional Southwest University adult lifespan dataset. *Scientific Data*, *5*, 180134.

West, K. L., Zuppichini, M. D., Turner, M. P., Sivakolundu, D. K., Zhao, Y., Abdelkarim, D., Spence, J. S., & Rypma, B. (2019). BOLD hemodynamic response function changes significantly with healthy aging. *NeuroImage*, *188*, 198–207.

Wingfield, A., & Grossman, M. (2006). Language and the aging brain: Patterns of neural compensation revealed by functional brain imaging. *Journal of Neurophysiology*, *96*(6), 2830–2839. https://doi.org/10.1152/jn.00628.2006

Wright, P. W., Brier, L. M., Bauer, A. Q., Baxter, G. A., Kraft, A. W., Reisman, M. D., Bice, A. R., Snyder, A. Z., Lee, J. M., & Culver, J. P. (2017). Functional connectivity structure of cortical calcium dynamics in anesthetized and awake mice. *PLoS One*, *12*(10), e0185759. https://doi.org/10.1371/journal.pone.0185759

Wu, C. W., Gu, H., Lu, H., Stein, E. A., Chen, J.-H., & Yang, Y. (2008). Frequency specificity of functional connectivity in brain networks. *NeuroImage*, *42*(3), 1047–1055. https://doi.org/10.1016/j.neuroimage.2008.05.035

Wu, G., Liao, W., Stramaglia, S., Ding, J., Chen, H., & Marinazzo, D. (2013). A blind deconvolution approach to recover effective connectivity brain networks from resting state fMRI data. *Medical Image Analysis*, *17*(3), 365–374.

Wu, G., Stramaglia, S., Chen, H., Liao, W., & Marinazzo, D. (2013). Mapping the voxel-wise effective connectome in resting state fMRI. *PLoS One*, *8*(9), e73670.

Wu, G. R., Colenbier, N., Van Den Bossche, S., Clauw, K., Johri, A., Tandon, M., & Marinazzo, D. (2021). rsHRF: A toolbox for resting-state HRF estimation and deconvolution. *NeuroImage*, *244*, 118591. https://doi.org/10.1016/j.neuroimage.2021.118591

Xia, Y., Chen, Q., Shi, L., Li, M., Gong, W., Chen, H., & Qiu, J. (2019). Tracking the dynamic functional connectivity structure of the human brain across the adult lifespan. *Human Brain Mapping*, *40*, 717–728.

Xie, Y. C., Chan, A. W., McGirr, A., Xue, S. C., Xiao, D. S., Zeng, H. K., & Murphy, T. H. (2016). Resolution of high-frequency mesoscale intracortical maps using the genetically encoded glutamate sensor iGluSnFR. *Journal of Neuroscience*, *36*(4), 1261–1272. https://doi.org/10.1523/Jneurosci.2744-15.2016

Yan, C. G., Craddock, R. C., Zuo, X.-N., Zang, Y.-F., & Milham, M. P. (2013). Standardizing the intrinsic brain: Towards robust measurement of inter-individual variation in 1000 functional connectomes. *NeuroImage*, *80*, 246–262.

Yan, C. G., Wang, X. D., Zuo, X. N., & Zang, Y. F. (2016). DPABI: Data processing & analysis for (resting-state) brain imaging. *Neuroinformatics*, *14*(3), 339–351. https://doi.org/10.1007/s12021-016-9299-4

Yang, A. C., Huang, C. C., Yeh, H. L., Liu, M. E., Hong, C. J., Tu, P. C., Chen, J. F., Huang, N. E., Peng, C. K., Lin, C. P., & Tsai, S. J. (2013). Complexity of spontaneous BOLD activity in default mode network is correlated with cognitive function in normal male elderly: A multiscale entropy analysis. *Neurobiology of Aging*, *34*(2), 428–438.

Yang, A. C., Tsai, S. J., Lin, C. P., Peng, C. K., & Huang, N. E. (2018). Frequency and amplitude modulation of resting-state fMRI signals and their functional relevance in normal aging. *Neurobiology of Aging*, *70*, 59–69.

Yang, G. J., Murray, J. D., Glasser, M., Pearlson, G. D., Krystal, J. H., Schleifer, C., Repovs, G., & Anticevic, A. (2017). Altered global signal topography in schizophrenia. *Cerebral Cortex*, *27*(11), 5156–5169. https://doi.org/10.1093/cercor/bhw297

Zeng, L., Wang, D., Fox, M. D., Sabuncu, M., Hu, D., Ge, M., Buckner, R. L., & Liu, H. (2014). Neurobiological basis of head motion in brain imaging. *Proceedings of the National Academy of Sciences*, *111*(16), 6058–6062.

Zhang, J., Huang, Z., Tumati, S., & Northoff, G. (2020). Rest-task modulation of fMRI-derived global signal topography is mediated by transient coactivation patterns. *PLoS Biology*, *18*(7), e3000733. https://doi.org/10.1371/journal.pbio.3000733

Zuo, X. N., Biswal, B. B., & Poldrack, R. A. (2019). Reliability and reproducibility in functional connectomics. *Frontiers in Neuroscience*, *13*, 117.

SUPPORTING INFORMATION

Additional supporting information can be found online in the Supporting Information section at the end of this article.

How to cite this article: Ao, Y., Yang, C., Drewes, J., Jiang, M., Huang, L., Jing, X., Northoff, G., & Wang, Y. (2023). Spatiotemporal dedifferentiation of the global brain signal topography along the adult lifespan. *Human Brain Mapping*, *44*(17), 5906–5918. https://doi.org/10.1002/hbm.26484